NCC3-1055

Particle Size Distributions Measured in the B757 Engine Plume During EXCAVATE

Terry Sanders, Paul Penko, Monica Rivera*, Steve Culler

NASA Glenn Research Center
*University of Toledo/NASA Glenn Research Center

Abstract

The Experiment to Characterize Aircraft Volatile Aerosols and Trace Species Emissions (EXCAVATE) took place at NASA Langley Research Center during January 2002. This ground based study was conducted to examine the role of fuel sulfur content on particulate emissions. Size distributions as a function of engine operating conditions were measured in the exhaust plume of a B-757 at four downstream axial locations (1 m, 10 m, 25 m and 35 m). The engine was run on JP-5 with three different sulfur concentrations, 810 ppm, 1050 ppm, 1820 ppm; and was operated over a range of power settings from idle to near-full power. Zalabsky differential-mobility analyzers (DMAs), Met One condensation-nuclei counters (CNCs), and a TSI 3022 condensation-particle counter (CPC) were used to measure the size distributions. The total number-count (particle concentration), number-based Emissions Index (EI_{number}) and mass-based Emissions Index (EI_{mass}) increased with fuel sulfur-content and engine pressure ratio (EPR). Count Mean Diameter (CMD) also increased with EPR yet remained fairly constant with fuel sulfur-content for a fixed location in the exhaust plume. Also the mode and CMD both increased with distance in the plume.

I. Introduction

Aircraft engines release over 750 million tons of pollutants into the environment per year.[1] The International Civil Aviation Organization (ICAO) estimates domestic aircraft contribute 3.5 thousand tons of pollutants annually in the form of solid particles.[2] Solid particles are composed mainly of soot and are nonvolatile. Though less than 1% of domestic aircraft emissions, these nonvolatile particles pose both health and environmental risks.[3] Current regulations limit the mass concentration of particles with diameters smaller than 2.5 μm ($PM_{2.5}$) that can be emitted from gas turbine engines. However, this regulation does not address particle number concentration.[4] For aircraft emissions the number concentration of volatile particles, assumed to be a mixture of sulfuric acid and water, is higher than the concentration of nonvolatile particles. Volatile particles may influence physical and chemical atmospheric processes e.g., increasing cloudiness and ozone depletion. Several experimental and modeling studies have shown a correlation between fuel sulfur-content and volatile particle emissions from aircraft.[5-9] The number of volatile particles emitted increases with higher fuel sulfur content and to date the amount of fuel sulfur converted within the engine or possibly within the exhaust plume remains unresolved, although estimates exist. No correlation between fuel sulfur content and nonvolatile particle concentration has been observed.[10-12] This report describes ground based measurements of particle size, and concentration in an engine plume as a function of fuel sulfur content, measurement location, and engine operating conditions.

II. Test Description

A ground-based test, the Experiment to Characterize Aircraft Volatile Aerosols and Trace Species Emissions (EXCAVATE), was conducted at NASA Langley Research Center, January 26 – 27, 2002, with a Boeing 757 aircraft. The aircraft was anchored on a tarmac and two probes were positioned downstream of the right-side engine, a Rolls Royce RB211-585. One probe was designed and fabricated by Arnold Engineering Development Center (AEDC) and had a 45.6 mm (1.794 in.) ID, Fig. 1. A second probe, constructed of 6.4 mm (0.25 in.) stainless-steel tubing at NASA Langley Research Center, had a 6 mm (0.22 in.) ID. The engine was run on JP-5 with three different sulfur concentrations, 810 ppm, 1050 ppm, 1820 ppm; and was operated over a range of power settings from idle to near-full power. Particulate size-distributions and concentrations were measured at four downstream axial locations: 1 m and 10 m with the AEDC particulate probe, and 25 m and 35 m with the Langley probe. Fuel with various sulfur contents was tested to address the long-standing question of the role of sulfur in the formation of volatile species. The object of EXCAVATE was to further study the effect of sulfur content on particulate number-concentration and size-distribution as a function of location in the engine plume and engine operating conditions.

III. Test Matrix

The test parameters are listed in Table 1. EPR is engine pressure-ratio which was varied from 1.03 (idle) to 1.5 (slightly less than take-off power). Dilution-ratio is the amount of dry, clean diluent added to the drawn exhaust-sample at the probe tip, and was calculated from the difference in carbon dioxide concentration between the exhaust-sample and diluted-sample. The JP-5 had an as-delivered sulfur-content of 810 ppm. Tetrahydrothiophene was blended with the JP-5 to obtain sulfur-concentrations of 1050 and 1820 ppm.

IV. System Description and Experimental Approach

A mobile lab, the Particulate and Gaseous Emissions Measurement System (PAGEMS), was used during EXCAVATE to measure particulate-emissions in the Boeing 757 engine-plume. Distributions of particulate number-concentrations from 10 nm to 450 nm were obtained using the equipment and hardware shown in Fig. 2. The measurement system included two Zalabsky differential-mobility analyzers (DMAs)[4], two Met One condensation-nuclei counters (CNCs), a TSI 3022 condensation-particle counter (CPC) (*CNC and CPC are trade names for the same type of instrument*), two stainless-steel 30-liter sample-storage tanks, a dew-point hygrometer, two filter-needle diluters, forty valves, and three vacuum pumps, one diaphragm and two vane pumps. Other components were an industrially-hardened computer, five ^{210}Po bi-polar chargers, several electrically-heated sample-transport lines, and thermocouples and pressure transducers. PAGEMS also has a suite of gaseous-emission analyzers that were not used in EXCAVATE and are not discussed here.

A custom-written LabVIEW program controlled the hardware and instrumentation for particle sampling and data acquisition via an Omega OM-1050 Remote Measurement and Control System. Temperatures, voltages, valve positions, pressures, relative humidity and flow rates were monitored by the OM-1050 and the data recorded every second.

Sample was extracted from the exhaust of the engine with the two probes previously described. The sample was diluted at the probe tip with dry nitrogen to reduce humidity, particle concentration and inhibit particle coagulation. The dilution-ratio, defined as

$$DR = \frac{TFR}{SFR} \tag{1}$$

where

TFR = undiluted sample flow rate + diluent flow rate, lpm
SFR = undiluted sample flow rate, lpm

varied from ~ 2:1 to 28:1 depending on engine condition and test parameter (see Table I). A common manifold with several tee-off points supplied sample to various research groups with a variety of measurement instruments. From this tee-off point a 30 m long electrically-heated line (6.25 mm OD) transported sample to PAGEMS. The line temperature was held to 180 C to prevent water-vapor condensation. On entering PAGEMS, the sample passed through a ^{210}Po bipolar charger exposing the particles to ions of plus and minus polarities to give them a known Boltzmann's charge distribution.

A fraction of the incoming sample, 1.5 liters per minute (lpm), was pulled into the TSI 3022 CPC. The CPC measured the total number-concentration of particulates in the diluted sample. This counter has an upper measurement limit of 10^7 particles/cc. To avoid exceeding this limit, a set of filter-needle diluters (FND) upstream of the TSI 3022 (see Fig. 2) further diluted the particle-concentrations by either 17:1 or 29:1. The design and construction of the FNDs are described in [13], and are essentially Whatman paper filters with hypodermic needles at the center of the filter. The diluters were calibrated to have a mean dilution-ratio over a range of particle sizes, in this case 10 nm – 450 nm.

The incoming sample was first stored in one of the 30-liter tanks. During a tank fill, the data acquisition system monitored the total number-concentration. Before filling with sample, the tank was purged for 3 minutes with dry particle-free air. For the range of plume particle-concentrations (10^5 to 10^7 particles/cc) encountered in EXCAVATE, a fill time of 3 – 5 minutes was required.

Following tank-fill, approximately 1.5 lpm of sample was drawn through another ^{210}Po bipolar charger then into a DMA. In the DMA, particles pass through a high-voltage electric field and the positively-charged particles are attracted to a negatively-charged center electrode. The electrode is surrounded by an annular-sheath of filtered air, at a rate of approximately 20 lpm, and has a small slit opening at the base. Depending on the voltage, particles with a certain electrical-mobility, and therefore size, migrate through the sheath air and exit through the slit. A Met One CNC downstream of the DMA measures the number-concentration of the mono-disperse aerosol from the DMA. Voltages were set on the center electrode to classify particles in the range of 10 nm to 450 nm. This process of classifying a particle sample with the DMA and counting the particles in the sample was termed a "sweep". The sweep data was then analyzed post-test to obtain the size distribution using an inversion algorithm provided by the University of Missouri-Rolla.[14] The total number-concentration was used in the inversion algorithm to normalize the measured size-distributions. More detailed information on the operating principles of the condensation-particle counters and differential-mobility analyzer, and their application in measuring particle-concentrations and size-distributions can be found in several texts.[15-16]

In the first phase of measurements, the AEDC particulate-probe was located at 1 m and the Langley probe at 25 m from the engine exit-plane. The aircraft was then moved forward about 9 m whereby the AEDC and Langley probes were at 10 m and 35 m, respectively, from the engine exit-plane. At both positions of the aircraft, the engine was operated over a range of pressure-ratios from idle (1.03 EPR) to near-full power (1.5 EPR) on fuel with each of three sulfur-concentrations: 810 ppm, 1050 ppm, and 1820 ppm. In all, particle measurements were made at 1 m, 10 m, 25 m, and 35 m downstream of the engine exit-plane. Dilution-ratios were varied, along with the other test parameters (see Table 1), and on average were about 9:1.

V. Discussion of Results

Because of computer malfunctions, a number of measurements for certain engine operating points and probe locations were missed. In the context of the total test matrix, the data set is incomplete. Furthermore, the measurement system does not distinguish volatile and non-volatile particles. Consequentially, all particles present in the sample that reached the measurement equipment were counted.

In regard to exhaust-sample dilution, a test for the effect of sample-dilution on particle-distributions and concentration (corrected for dilution) was conducted at the University of Minnesota in July of 2003. An important result from that exercise was that probe and line losses reach a minimum at a dilution-ratio of ~8:1. For a dilution-ratio of 6:1, there was 2-5% greater loss, depending on particle size, than for the 8:1 dilution-ratio. Based on these findings, the EXCAVATE data for dilution-ratios less than about 6:1 were not considered.

The EXCAVATE test points are listed in Table 1. Each point has a run number and is described in terms of engine pressure-ratio (EPR), probe-location, fuel sulfur-content and dilution-ratio. Each point has an associated sweep-number specific to PAGEMS. Table 2 contains statistical information on the particle size-distributions for all the test points. The statistics were calculated using the Hatch-Choate equations from Hinds.[8] The data from the 1-m probe-location are the most complete and results are drawn primarily from this set. Particle-distributions for the 1-m probe-location are plotted in Figs. 3, 4, 5, and 8 for various EPRs and fuel sulfur-concentrations. Fig. 6 is for a probe location of 25 m and Fig. 7, for probe-locations of 1 m and 25 m. Count mean-diameter (CMD) as a function of fuel sulfur-concentration and EPR are plotted in Figs. 9 and10. It should be noted that the particle-distribution measurements were repeatable for given test points e.g., fixed probe distance, fuel sulfur content and EPR (Appendix B).

For the data at the 1-m probe-location:

1. In Fig. 3, fuel sulfur-content is 810 ppm. For an EPR of 1.03 the mode is ~15 nm. At an EPR of 1.3, the mode is shifted by a factor-of-two to 31 nm.
2. In Fig. 4 a shift in mode occurs as a function of EPR. For an EPR of 1.15, the mode is ~21 nm and, for 1.3, is ~ 28 nm.
3. In Fig. 5, sulfur content is 1820 ppm and the parameter is EPR. The mode shifts from ~25 nm at an EPR of 1.15 to ~35 nm for an EPR of 1.4.
4. For the size distributions plotted in Fig. 8, the mode remains about constant at ~30 nm for varying sulfur-content from 810 ppm to 1820 ppm at a constant EPR of 1.3.
5. In Fig. 9, the CMD increases from ~35 nm to ~55 nm over a range of EPR from 1.15 to 1.5 for a constant fuel sulfur-content of 1820 ppm.
6. In Fig. 10, the CMD remains about constant for a fuel sulfur-concentration ranging from 810 ppm to 1820 ppm and a fixed EPR of 1.3.

For the 25-m probe-location:

1. In Fig. 6, the CMD of the distributions is ~53 nm, indicating an increase in particle-size with distance in the plume from 1 m to 25 m.
2. In Fig. 7, there is a shift in mode with probe-location from ~28 nm at 1 m to ~40 nm at 25 m.

Results for the integrated values of the distributions, i.e. total number-count, number-based emission-index (EI_{number}) and mass-based emission-index (EI_{mass}) are given in Figs. 9 -14. The number- and mass-based emission-indices normalize the total particle-count and particle-mass for fuel burn-rate. The equation for number- and mass-based emission-indices is:

$$EI(X) = \left(\frac{\Delta X}{\Delta CO_2}\right) * EI(CO_2) * \left(\frac{M_{air}}{\rho_{air} * M_{CO_2}}\right) \qquad \frac{g}{kg\ fuel} \qquad (2)$$

ΔX = mass or number of particulate matter/unit volume of exhaust, above ambient, g/cc or #/cc

ΔCO_2 = concentration of CO_2 in exhaust above ambient, volume fraction

$EI(CO_2)$ = emission index of CO_2, ~ 3160 g/kg fuel burned
M_{air} = molecular mass of air, 29 kg/kmol
M_{co2} = molecular mass of CO_2, 44 kg/kmol
ρ_{air} = density of air, 1.295 g/cc for P_{std} = 101.326 kPa, T_{std} = 273 K

Particle-mass is calculated from the number distributions assuming that the particles are spherical and their density is 1 g/cc.

For the integrated values of the distributions:

1. Fig. 11 shows the change in total number-count as a function of EPR for a probe-position of 1 m and sulfur-content of 1820 ppm. There is a trend of increasing number count with EPR, ranging from about 1.86 $x10^7$ #/cc at an EPR of 1.15 to 2.09 $x10^7$ #/cc at an EPR of 1.4.
2. Fig. 12 is a plot of total number-count as a function of fuel sulfur-content for a probe-position of 1 m and EPR of 1.3. The number-count changes about an order-of-magnitude for a doubling of sulfur-content, ranging from 2.79 $x10^6$ #/cc at a sulfur-concentration of 810 ppm, to 1.84 $x10^7$ #/cc for a sulfur-concentration of 1820 ppm.
3. In Fig. 13, the results for EI_{number} show a different trend than total number count with EPR, with the highest value occurring at an EPR of 1.15.
4. In Fig. 14, the EI_{number} shows a trend similar to the total-number count as a function of fuel sulfur-content.
5. The EI_{mass}, plotted as a function of EPR in Fig. 15, has a minimum at an EPR of 1.15. This occurs because the count mean-diameter is smaller for an EPR of 1.15 than it is for higher EPRs.
6. The EI_{mass} as a function of sulfur-content, Fig. 16, shows a similar trend as the EI_{number} in Fig. 14.

VI. Experimental Uncertainty

Two components of experimental uncertainty are addressed. The first type, commonly known as systemic error, entails diffusional particle loss in the sample transport line and DMA. Diffusional loss in the transport line is termed line-transmission efficiency and diffusional loss in the DMA, DMA efficiency. Particle loss in the transport line is a function of flow rate, line diameter, and density of the aerosol medium, expressed as Reynolds Number; and line length and particle size. For this test, Reynolds Numbers were $< 2 \times 10^3$, with the flow largely laminar. Calculated transmission efficiencies due to diffusional losses, for 30.5 m (100 ft.) of 6.4 mm (0.25 in.) tube heated to 180 C (350 F), vary from about 50% for a particle size of 10 nm to nearly 97% for particles > 100 nm. Please refer to Appendix C for equations used to model diffusive deposition transport efficiencies i.e. diffusional losses. DMA efficiency is from ref. [8] and is 3%. The data presented in this report are not corrected for transmission-line or DMA losses.

Uncertainty in the data, i.e. precision error, is given as the upper and lower values of quantities calculated from the size distributions such as total number-count or EI. In most cases, a sufficient number of data points at a given condition are not available for standard statistical analysis, e.g. standard deviation. Plotted values are the mean of the calculated quantities for test conditions where there is more than one data point. In some cases, only one data point is available and is presented with no uncertainty bar.

VII. Summary

In general, total number-count, number-based EI and mass-based EI increase with fuel sulfur-content and EPR. CMD increases with EPR but is about constant with fuel sulfur-content for a fixed location in the exhaust plume. The limited comparison of the particle-distributions at the 1-m and 25-m probe-locations indicates that the mode and CMD both increase with distance in the plume.

Unfortunately, problems encountered with the equipment did not allow measurement of particle-distributions at all test points. In particular, data at various probe-locations in the engine-plume, other than 1 m, are sparse. Furthermore, there is no distinction in the data between volatile and nonvolatile particle number-concentrations.

Acknowledgments

The contribution of Alexia Finotello, Summer Intern, is greatly appreciated in the analysis and archiving of the data. The EXCAVATE Project was organized and funded by the UEET Project Office, Dr. Chowen Wey, Project Manager. Her encouragement and support are most appreciated.

VIII. References

1. L.J. Archer, *Aircraft Emissions and the Environment*, Oxford Institute for Energy Studies, 1993.
2. Corporan, E., DeWitt, M., and Wagner, M., "Evaluation of Soot Particulate Mitigation Additives in a T63 Engine", Proceedings of the International Conference on Air Quality III, September 10-12, 2002.
3. Seinfeld, J. H. and Pandis, S. N., *Atmospheric Chemistry and Physics*; Wiley: New York, 1998.
4. Morawska, L., Johnson, G., Ristovski, Z.D., and Agranovski, V., "Relation between Particle Mass and Number for Submicrometer Airborne Particles", Atmospheric Environment, Vol. 33, pp. 1983- 1990, 1999.
5. Brown, R.C., Anderson, M.R., Miake-Lye, R.C., and Kolb, C.E., "Aircraft Exhaust Sulfur Emissions", Geophys. Res. Lett. Vol. 23, pp. 3603-3606, 1996.
6. Fahey, D.W. *et al.*, "Emission Measurements of the Concorde Supersonic Aircraft in the Lower Stratosphere", Science Vol. 270, pp. 70-74, 1995.
7. Karcher, B., Peter, Th., Biermann, U.M., and Schumann, U., "The Initial Composition of Jet Condensation Trails", J. Atmos. Sci., Vol. 53, pp. 3066-3083, 1996.
8. Schmid, O., Tandem Differential Mobility Analyzer Studies and Aerosol Volatility, Ph.D. Thesis, University of Missouri, Rolla, Missouri, 2000.
9. Schumann, U., Strom, J., Busen, R., Baumann, R., Gierens, K., Krautstrunk, M., Schroder, F.P., and Stingl, J., "In Situ Observations of Particles in Jet Aircraft Exhaust and Contrails for Different Sulfur-Containing Fuels", J. Geophys. Res., 101, pp. 6853-6869, 1996.
10. Whitefield, P.D. *et al.*,"NASA/QinetiQ Collaborative Program – Final Report", NASA/CR-2002-211900.
11. Sorokin, A., Katragkou, E., Arnold, F., Busen, R., and Schumann, U., "Gaseous SO_3 and H_2SO_4 in the Exhaust of an Aircraft Gas Turbine Engine: Measurements by CIMS and Implications for Fuel Sulfur Conversion to Sulfur (VI) and

Conversion of SO_3 to H_2SO_4", Atmospheric Environment Vol. 38, pp. 449-456 2004.
12. Schumann, U. *et al.*, "Influence of Fuel Sulfur on the Composition of Aircraft Exhaust Plumes: The Experiments SULFUR 1-7", J. Geophys. Res., 107, pp. 2-1 – 2-27, 2002.
13. Olson, D.D., Trueblood, M.B., and Whitefield, P.D., "The Development of a Novel Dilution Technique for Sub-micron Particulate Characterization", OURE Program Report, University of Missouri-Rolla, 1996.
14. Hagen, D. E., and Alofs, D. J., "A Linear Inversion Method to Obtain Aerosol Size distributions from Measurements with a Differential Mobility Analyzer", Aerosol Science and Technology, Vol. 2, pp. 465-475, 1983.
15. Hinds, W. C. *Aerosol Technology;* Wiley: New York, 1999.
16. Willeke, K., and Baron, P.A., *Aerosol Measurement*;Van Nostrand Reinhold: NewYork, 1993.

IX. Appendix A: Hardware dimensions and system parameters

Dimensions of the Zalabsky Differential Mobility Analyzers used for the EXCAVATE tests.

Rod O.D., cm	Cylinder I.D., cm	Length, cm
r =4.445	r =2.540	72.77

Flow rates through the DMA and the high voltage range used in the measurements.

DMA aerosol flow rate, lpm	DMA sheath flow rate, lpm	Initial DMA sweep Voltage, V	Final DMA sweep Voltage, V
1.5	20	17.5	14, 532

X. Appendix B: Repeatability measurements

In order to determine if the particulate-sizing equipment calibration drifted with time repeat measurements were made at given test points e.g., fixed probe distance, fuel sulfur content and EPR. It was observed that the size distribution measurements were repeatable indicating negligible equipment calibration drift.

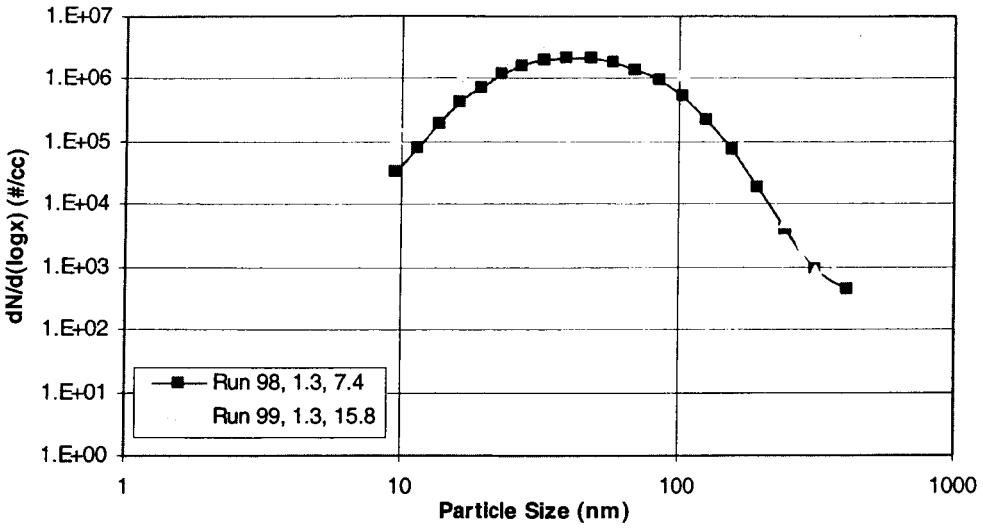

Fig. B1. Particle size distributions for a constant probe distance (1m), fuel sulfur content (810 ppm) and EPR (1.3); parameter is dilution ratio.

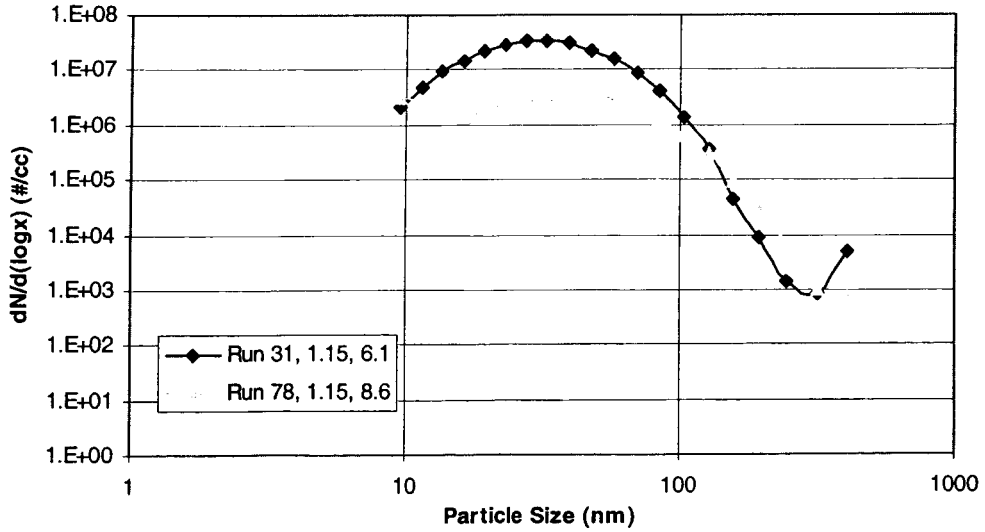

Fig. B2. Particle size distributions, for a constant probe distance (1m), fuel sulfur content (1050 ppm) and EPR (1.15); parameter is dilution ratio.

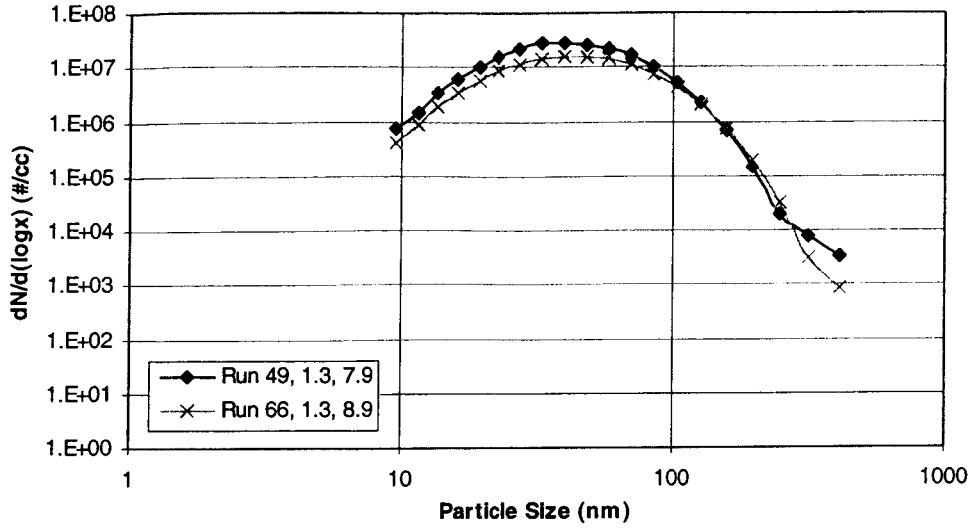

Fig. B3. Particle size distributions, for a constant probe distance (1m), fuel sulfur content (1820 ppm) and EPR (1.3); parameter is dilution ratio.

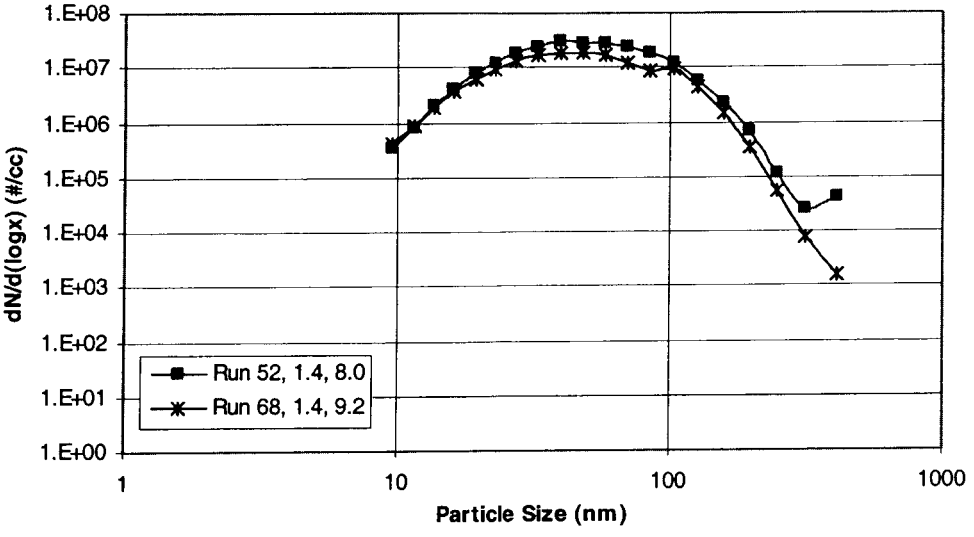

Fig. B4. Particle size distributions, for a constant probe distance (1m), fuel sulfur content (1820 ppm) and EPR (1.4); parameter is dilution ratio.

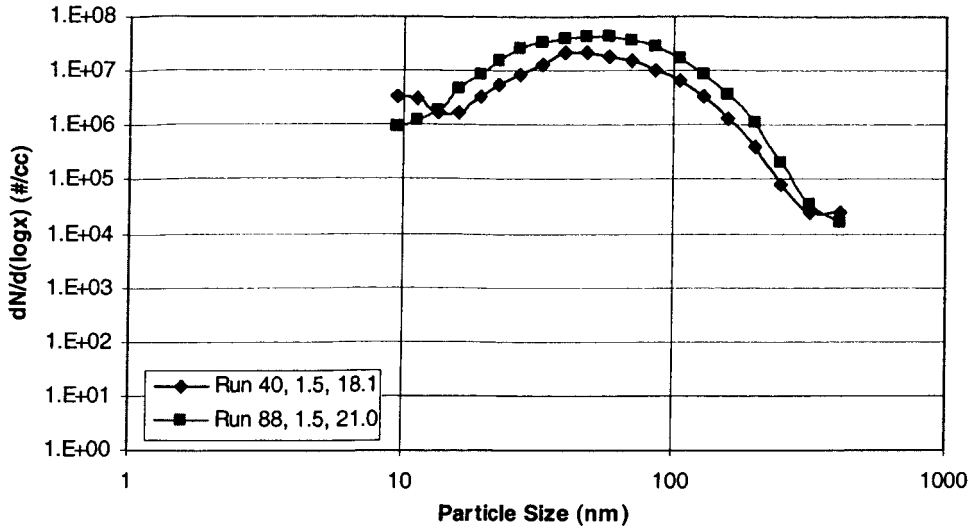

Fig. B5. Particle size distributions, for a constant probe distance (25m), fuel sulfur content (1050 ppm) and EPR (1.5); parameter is dilution ratio.

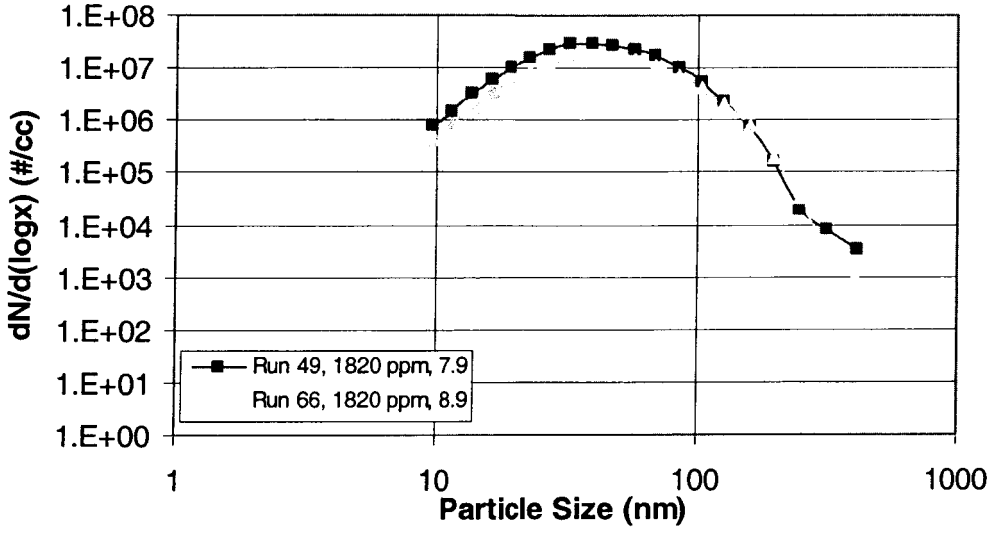

Fig. B6. Particle size distributions, for a constant probe distance (1m), fuel sulfur content (1820 ppm) and EPR (1.3); parameter is dilution ratio.

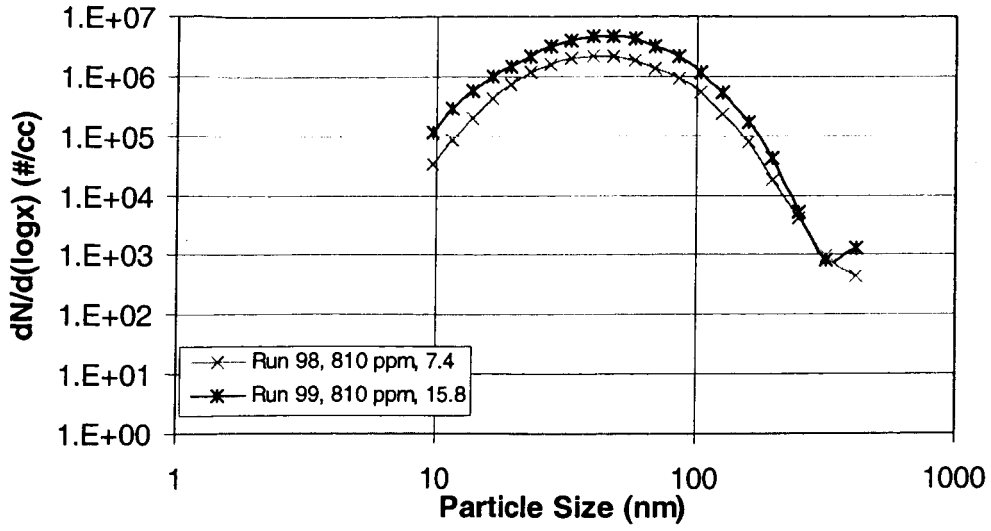

Fig. B7. Particle size distributions, for a constant probe distance (1m), fuel sulfur content (810 ppm) and EPR (1.3); parameter is dilution ratio.

XI. Appendix C: Diffusive deposition transport efficiency

Particle loss during transport is the result of several deposition mechanisms [16]. For the experimental setup used in EXCAVATE, all deposition mechanisms except diffusive deposition were assumed to be negligible. In order to theoretically assess particle loss due to diffusion, a model was created from equations found in Willeke & Baron. Particle diameters, gas properties such as temperature, and pressure, tube length, tube diameter, and volumetric flow rate through the tube are inputs to the model. For the model the following assumptions were used 1) nonvolatile particles 2) negligible coagulation and 3) laminar tube flow.

The Reynolds number (Re) inside the tube is given by Eqn 3-1 p.24

$$\mathrm{Re} = \rho g V1 * \frac{dia1}{\eta}, \tag{C1}$$

where ρg is the gas density in g/cm^3, V1 is gas velocity through tube in cm/s, dia1 is tube diameter in cm, and ηis the gas viscosity in dyn s/cm^2.

The mean free path (λ) in microns is given by Eqn 3-6 p. 26

$$\lambda = \lambda r * \left(\frac{101.3}{P}\right) * \left(\frac{T}{293.15}\right) * \left[\frac{\left(1+\frac{110}{293.15}\right)}{\left(1+\frac{110}{T}\right)}\right] \tag{C2}$$

λr, the mean free path reference value, is 0.0665 microns for air at 20 C (273.15 K) and 1 atm (101.3 kPa). T and P are the gas temperature and pressure in K and kPa, respectively.

The Knudsen number as a function of particle diameter (Kn(dia)) is given by Eqn 3-7 p.27

$$Kn(dia) = 2 * \frac{\lambda}{dp(dia)}, \tag{C3}$$

where dp(dia) is the particle diameter in microns.

The Cunningham slip correction factor as a function of particle diameter (Cc(dia)) is given by Eqn 3-8 p. 27

$$Cc(dia) = 1 + Kn(dia) * \left[\alpha + \beta * e^{\left(\frac{-\gamma}{Kn(dia)} \right)} \right], \tag{C4}$$

where α, β, γ are the slip coefficient constants for solid particles p.27
($\alpha = 1.142$, $\beta = 0.558$, $\gamma = 0.999$).

The definition of particle mobility as a function of particle diameter (B(dia)) (Eqn 3-14 p. 28) is then

$$B(dia) = \frac{Cc(dia)}{(3 * \pi * \eta * dp(dia))} \qquad \frac{cm}{s * dyn}, \tag{C5}$$

where dp(dia) is the particle diameter in centimeters.

Diffusivity as a function of particle diameter (D1(dia)) is given by Eqn 3-13 p. 28

$$D1(dia) = k * T * B(dia) \qquad \frac{cm^2}{s}, \tag{C6}$$

where k, the Boltzmann constant, is 1.38e-16 dyn cm/K.

The definition of ζ (dia) is given by Eqn 6-44 p. 97

$$\zeta(dia) = \pi * D1(dia) * \frac{L1}{Q2}, \tag{C7}$$

where L1 is tube length in cm, and Q2 is the volumetric flow rate through the tube in cm^3/s.

The transport efficiency as a function of particle size (η(dia)) in laminar tube flow for particles undergoing diffusive deposition is given by the Gormley and Kennedy (1949) equation (Eqn 6-46 p. 98)

for ζ (dia) < 0.02 (Eqn 6-46a)

$$\eta(dia) = 1 - 2.56 * \zeta(dia)^{\frac{2}{3}} + 1.2 * \zeta(dia) + 0.77 * \zeta(dia)^{\frac{4}{3}} \quad \text{(C8)}$$

for ζ (dia) > 0.02 (Eqn 6-46b)

$$\eta(dia) = 0.819 * \left[e^{(-3.657 * \zeta(dia))}\right] + 0.097 * \left[e^{(-22.3 * \zeta(dia))}\right] + 0.032 * e^{(-57 * \zeta(dia))} \quad \text{(C9)}$$

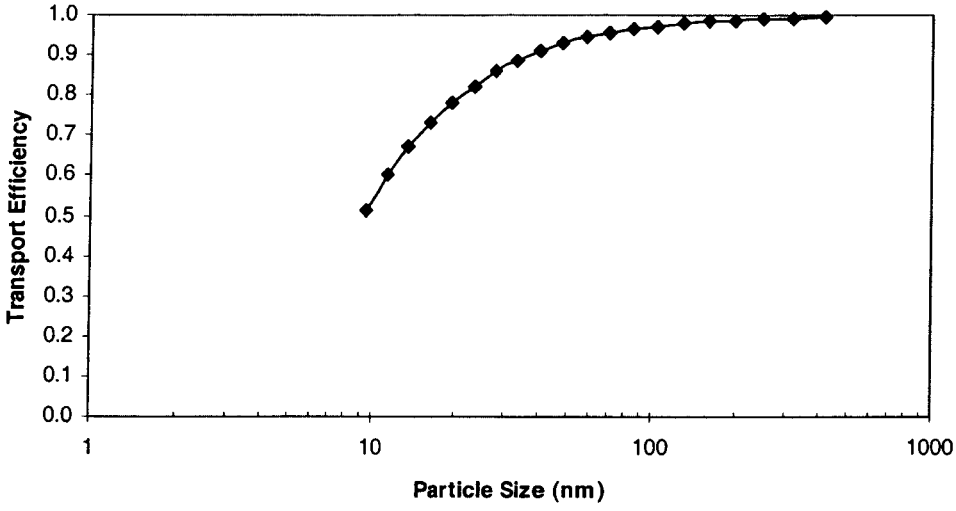

Fig. C1. Diffusive deposition transport efficiency as a function of particle size (η(dia)). The transfer line is a 6.4 mm (0.25 in.) diameter tube, 30.5 m (100 ft) long, heated to 180 C (350 F). Volumetric flow rate through the tube is 5 lpm and pressure is 1 atm.

XII. Appendix D: EXCAVATE Photographs

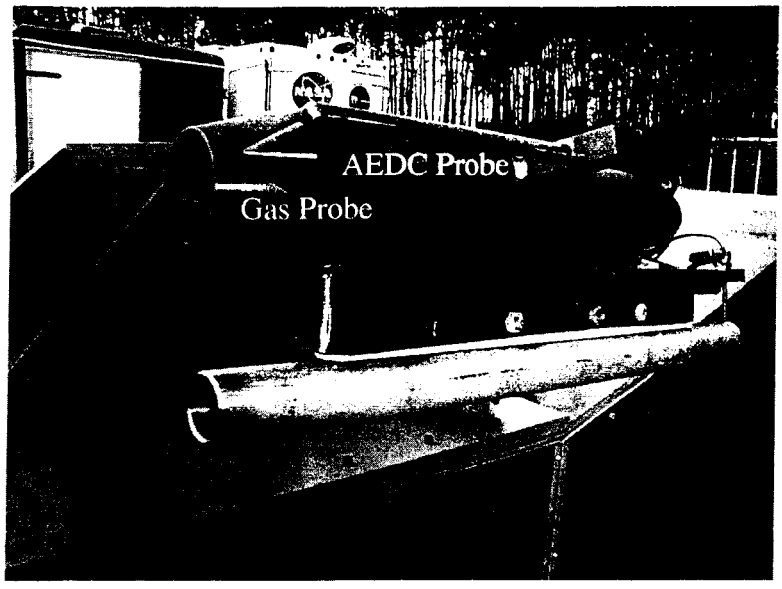

Fig. D1. Probes used in EXCAVATE

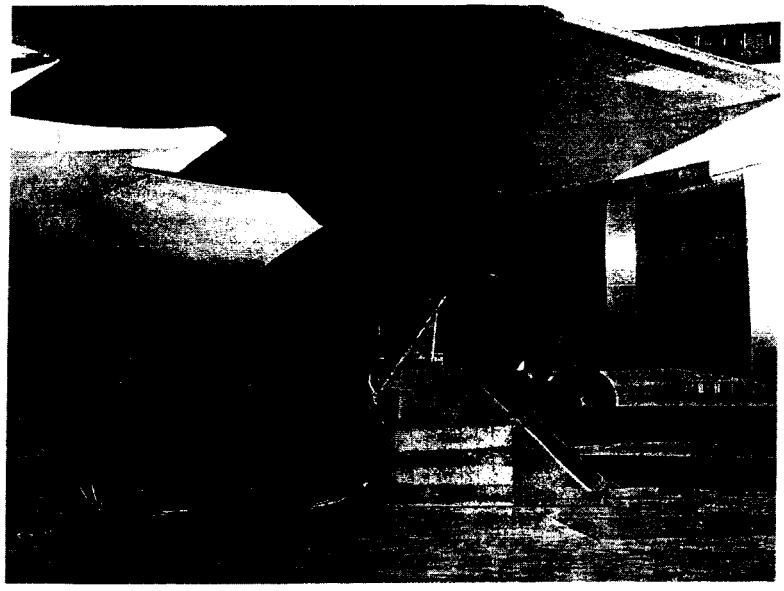

Fig. D2. Probes located 1-m behind Boeing 757 aircraft engine

Table 1. EXCAVATE Test Parameters

Run Number	EPR	Probe Location, m	Fuel Sulfur, ppm	Dilution Ratio	Sweep Number
31	1.15	1	1050	6.14	13
33	1.3	1	1050	7.15	14
33	1.3	1	1050	7.15	15
31	1.15	1	1050	6.14	16
37	1.4	25	1050	17.24	17
40	1.5	25	1050	18.1	18
40	1.5	25	1050	18.1	19
43	1.03	1	1820	4.52	20
46	1.15	1	1820	7.97	21
46	1.15	1	1820	7.97	22
49	1.3	1	1820	7.96	23
49	1.3	1	1820	7.96	24
52	1.4	1	1820	8.09	25
53	1.4	25	1820	20.23	26
56	1.03	25	1820	28.74	27
60	1.03	1	1820	4.55	01
63	1.15	1	1820	9.44	02
63	1.15	1	1820	9.44	03
66	1.3	1	1820	8.95	04
68	1.4	1	1820	9.29	05
69	1.4	1	1820	11.46	06
71	1.5	1	1820	10.67	07
78	1.15	1	1050	8.68	08
78	1.15	1	1050	8.68	09
82	1.3	25	1050	22.67	10
84	1.4	1	1050	9.29	11
88	1.5	25	1050	21.01	12
93	1.03	1	810	5.04	28
97	1.03	1	810	11.28	29
98	1.3	1	810	7.44	30
99	1.3	1	810	15.84	31
102	1.03	10	1050	1.6	32
103	1.03	10	1050	1.98	33
105	1.15	35	1050	2.99	34
108	1.3	10	1050	3.39	35
109	1.3	35	1050	3.88	36
109	1.3	35	1050	3.88	37
115	1.03	10	1820	2.38	38
115	1.03	10	1820	2.38	39
118	1.15	10	1820	3.52	40
121	1.3	10	1820	4.36	41
124	1.4	35	1820	6.15	42
124	1.4	35	1820	6.15	43
127	1.03	10	810	2.08	44
130	1.15	10	810	2.34	45
133	1.3	10	810	3.47	46
137	1.4	35	810	4.5	47
139	1.03	35	1820	2.89	48
141	1.15	10	1820	2.51	49
145	1.3	35	1820	3.87	50

Table 2. EXCAVATE Statistical Data

Run Number	Sweep Number	Standard Deviation	Geometric Standard Deviation	Count Median Dia., nm	Mode nm	Count Mean Dia., nm	Average Mass Dia., nm	Mass Median Dia., nm	Mass Mean Dia., nm	Mass EI g/kg fuel	Number EI #/kg fuel
31	13	17.3	1.1	30	23	33	42	61	68	6.02E-06	1.51E+16
33	14	23.0	1.2	37	28	42	55	83	95	2.66E-06	3.09E+15
33	15	25.3	1.2	40	30	46	60	92	106	3.46E-06	3.09E+15
31	16	28.4	1.1	47	36	53	69	102	116	5.03E-06	2.91E+15
37	17	30.9	1.4	22	12	30	58	151	208	2.12E-05	1.92E+16
40	18	30.4	1.2	44	30	53	77	134	162	2.90E-05	1.65E+16
40	19	31.0	1.2	43	28	53	81	153	188	2.95E-05	1.65E+16
43	20	36.6	1.2	49	34	58	84	143	171	1.31E-05	4.57E+15
46	21	22.6	1.3	19	12	23	37	76	96	7.89E-06	1.55E+16
46	22	17.9	1.2	18	12	23	34	62	77	3.88E-06	1.55E+16
49	23	24.2	1.1	39	30	44	58	87	99	1.18E-05	1.18E+16
49	24	26.5	1.2	40	30	46	62	96	111	1.45E-05	1.18E+16
52	25	30.5	1.2	46	35	54	72	112	129	2.16E-05	1.15E+16
53	26	32.1	1.2	48	35	56	76	122	142	1.53E-04	7.23E+16
56	27	31.9	1.2	50	38	58	78	121	140	3.25E-04	1.39E+17
60	1	45.5	1.4	33	17	46	90	248	347	4.66E-05	1.31E+16
63	2	21.9	1.2	33	25	39	52	82	95	6.11E-06	8.82E+15
63	3	22.0	1.2	35	26	40	54	83	96	6.40E-06	8.82E+15
66	4	27.4	1.2	41	30	48	65	101	118	9.49E-06	7.22E+15
68	5	30.9	1.2	44	31	51	71	116	137	1.59E-05	9.27E+15
69	6	29.6	1.2	44	33	51	70	110	128	1.98E-05	1.20E+16
71	7	31.9	1.2	47	35	55	75	119	138	2.91E-06	1.41E+16
78	8	25.6	1.3	27	16	35	58	126	162	1.96E-06	2.64E+15
78	9	25.7	1.3	30	19	37	58	114	142	2.13E-06	2.64E+15
82	10	30.7	1.1	52	40	59	76	111	126	2.94E-05	1.35E+16
84	11	29.8	1.2	44	32	52	71	112	131	5.48E-06	3.26E+15
88	12	30.5	1.2	48	36	55	74	113	130	6.96E-05	3.60E+16
93	28	20.0	1.2	26	20	30	40	61	70	3.07E-07	5.82E+14
97	29	23.3	1.3	24	15	30	48	95	120	1.25E-06	2.34E+15
98	30	26.1	1.2	41	31	47	62	93	107	1.05E-06	8.70E+14
99	31	26.4	1.2	41	30	48	65	103	119	4.88E-06	3.93E+15
102	32	21.4	1.3	18	12	23	36	69	85	3.25E-07	8.30E+14
103	33	9.6	1.1	12	11	13	14	16	17	1.43E-07	1.46E+15
105	34	7.5	1.0	14	12	14	15	17	18	1.17E-07	2.07E+15
108	35	28.1	1.2	39	27	46	67	116	139	1.91E-06	1.48E+15
109	36	30.6	1.3	33	21	42	69	141	180	2.54E-06	1.90E+15
109	37	30.7	1.3	34	22	43	68	135	170	2.67E-06	1.90E+15
115	38	56.4	1.5	39	17	60	140	500	763	9.87E-06	1.66E+15
115	39	44.7	1.5	21	9	32	74	260	395	5.36E-06	1.66E+15
118	40	27.4	1.2	35	24	41	59	100	120	3.04E-06	2.58E+15
121	41	28.6	1.2	44	33	51	68	105	122	3.61E-06	2.36E+15
124	42	31.3	1.2	45	33	52	71	112	130	6.48E-06	3.49E+15
124	43	32.0	1.5	24	11	36	77	245	360	4.35E-06	3.49E+15
127	44	30.9	1.2	47	35	55	73	114	132	2.58E-06	1.30E+15
130	45	25.0	1.1	41	32	46	59	85	96	1.28E-06	1.10E+15
133	46	28.8	1.2	41	30	48	67	109	128	2.18E-06	1.50E+15
137	47	36.2	1.2	50	37	58	79	123	143	5.61E-06	1.90E+15
139	48	16.9	1.1	14	11	16	21	30	33	8.38E-07	3.18E+15
141	49	24.0	1.1	39	30	44	56	81	92	1.30E-06	1.29E+15
145	50	29.3	1.2	46	34	52	70	106	123	3.11E-06	1.82E+15

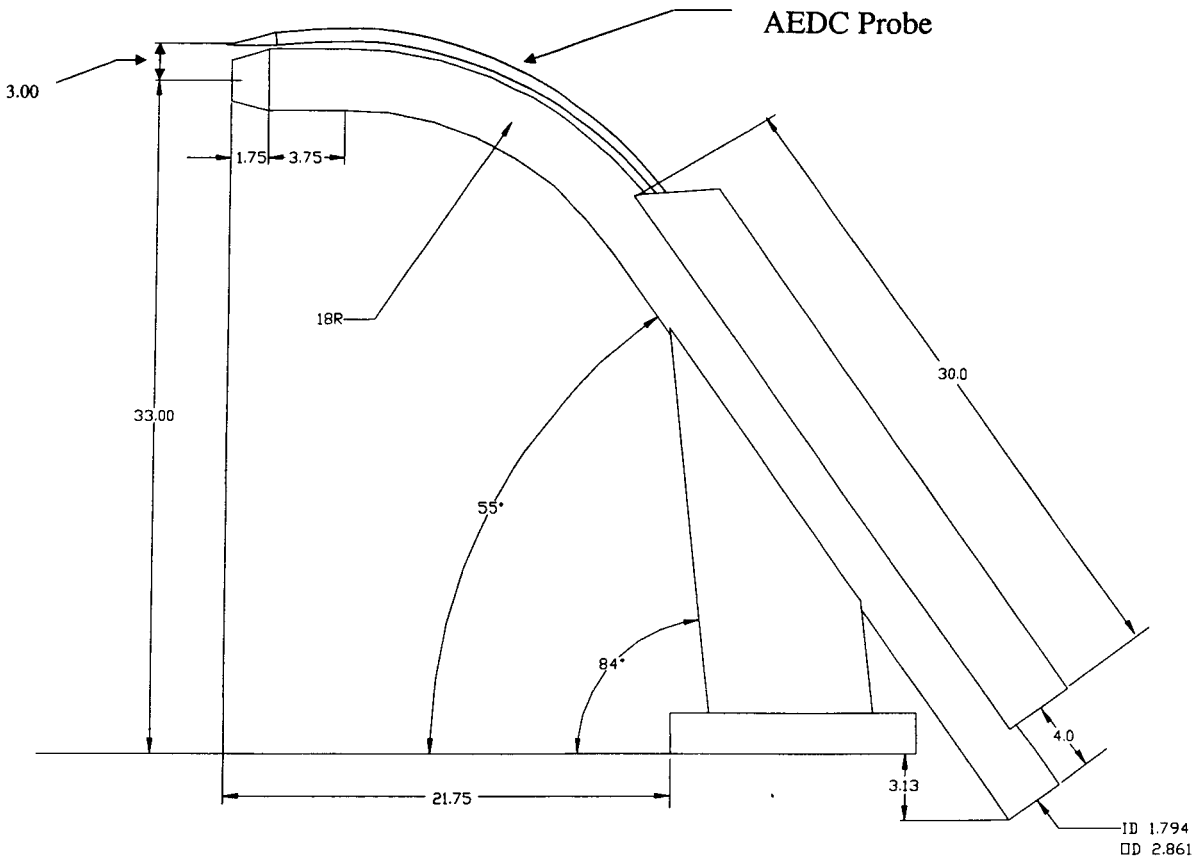

Fig. 1. AEDC particulate probe (dimensions are in inches).

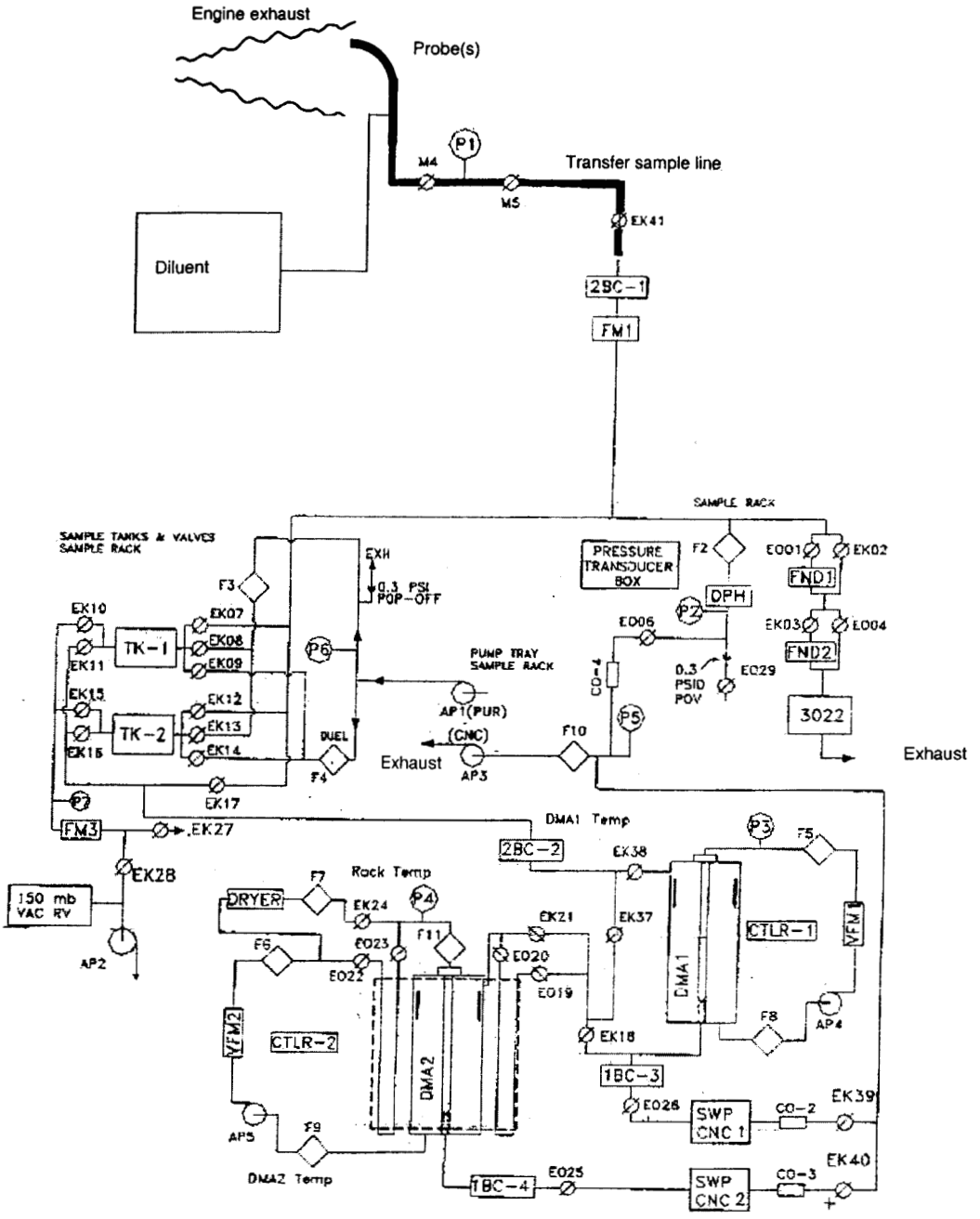

Fig. 2. Layout of Particulate and Gaseous Emissions Measurement System.
BC – bipolar charger, FM# - mass flow meter, FND# - filter needle diluter, DPH – dew point hygrometer, TK# - sample storage tank, AP# - vacuum pump, DMA# - differential mobility analyzer, SWP CNC# - sweep condensation nuclei counter, 3022 – TSI 3022 condensation particle counter, F# - filter, P# - pressure transducer, EK – normally closed solenoid valve, EO – normally opened solenoid valve, MV# - manual valve, CO# - critical orifice, CTRL# - controller, VFM# - volumetric flow meter

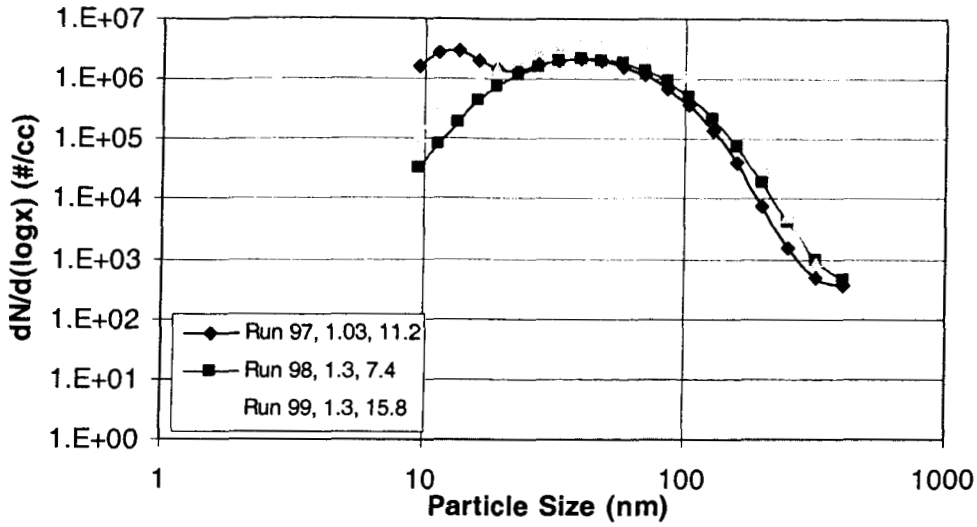

Fig. 3. Particle size distributions, probe distance 1 m, fuel sulfur content 810 ppm; parameters are engine pressure ratio and dilution ratio.

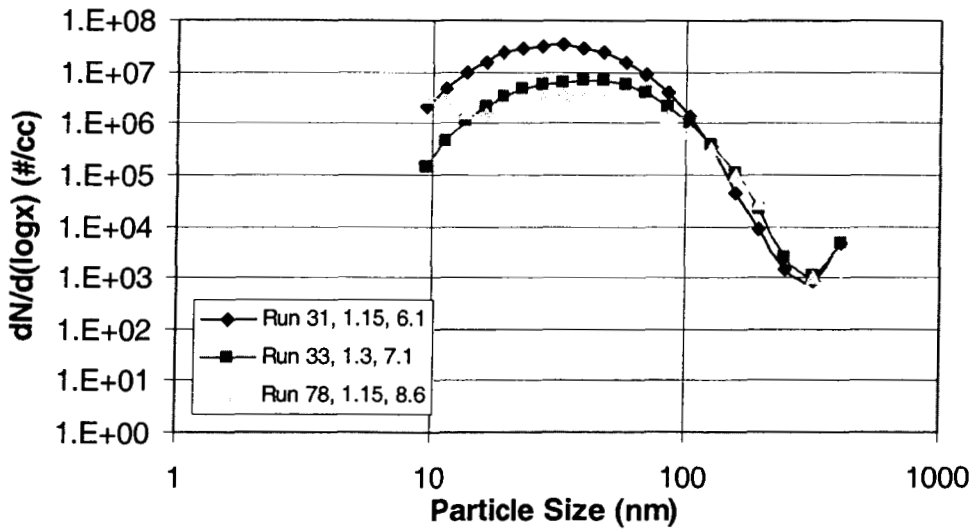

Fig. 4. Particle size distributions, probe distance 1 m, fuel sulfur content 1050 ppm; parameters are engine pressure ratio and dilution ratio.

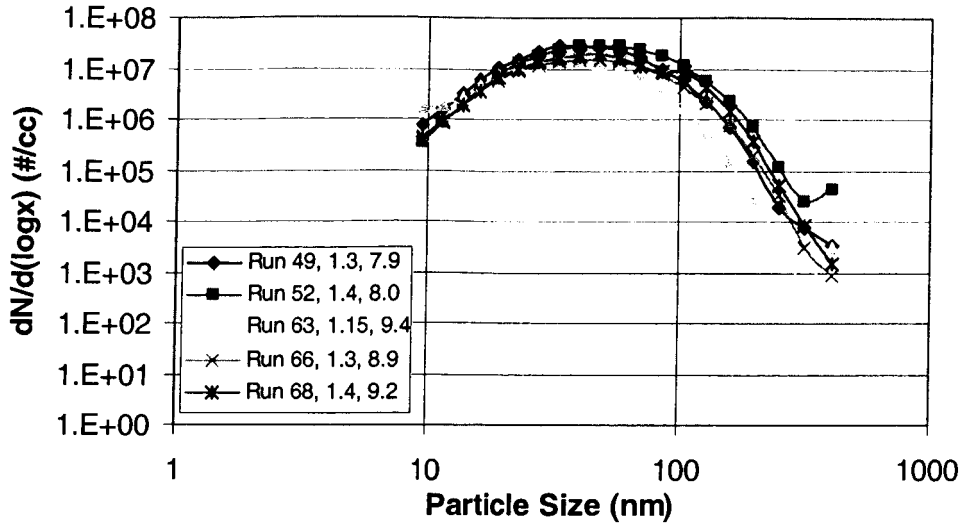

Fig. 5. Particle size distributions, probe distance 1 m, fuel sulfur content 1820 ppm; parameters are engine pressure ratio and dilution ratio.

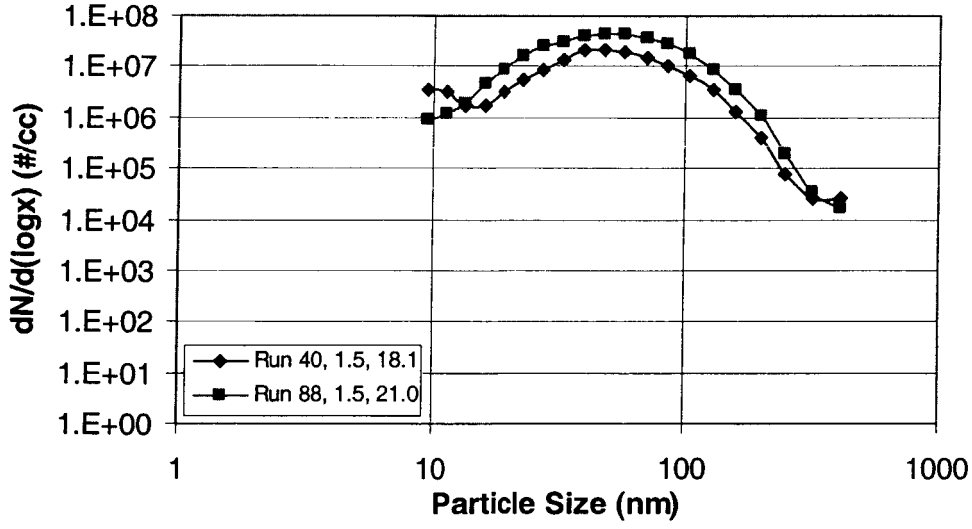

Fig. 6. Particle size distributions, probe distance 25 m, fuel sulfur content 1050 ppm; parameters are engine pressure ratio and dilution ratio.

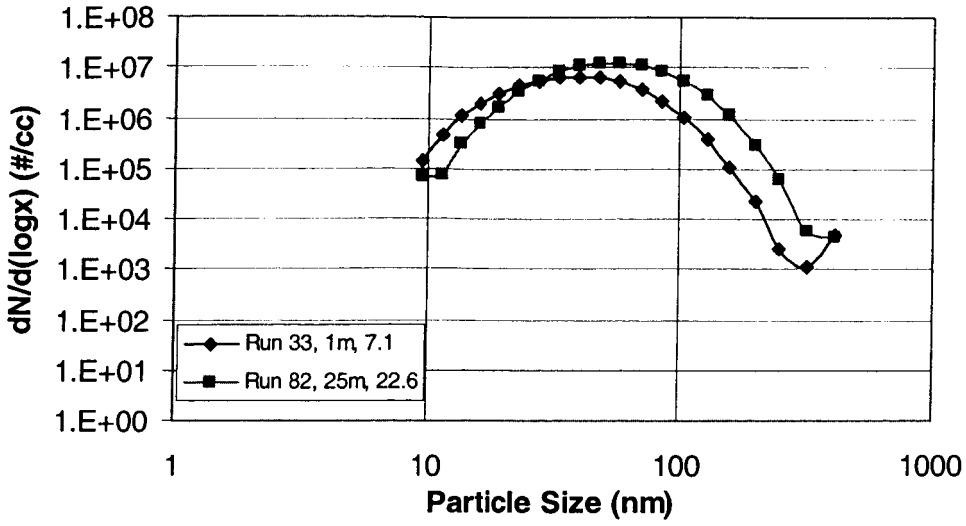

Fig. 7. Particle size distributions, engine pressure ratio 1.3, fuel sulfur content 1050 ppm, parameters are probe distance and dilution ratio.

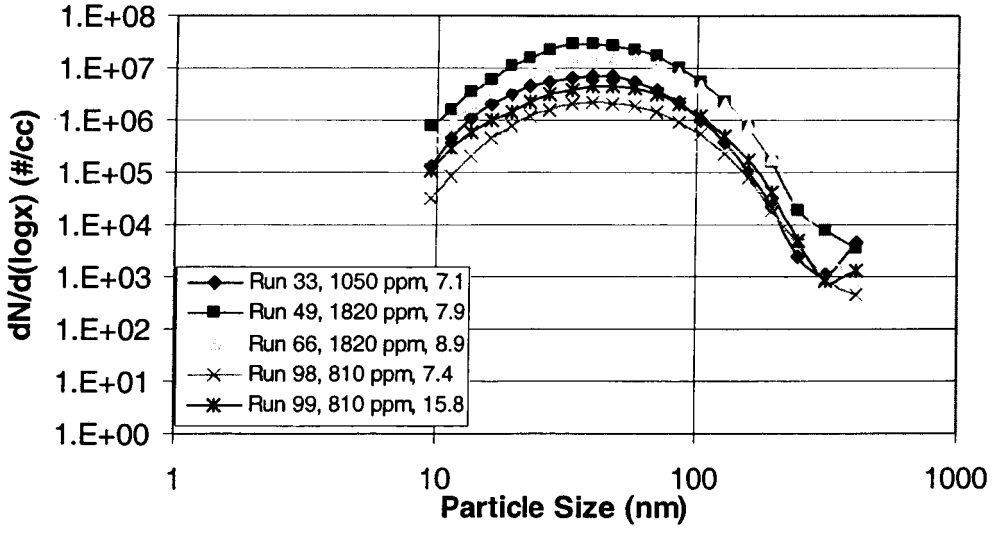

Fig. 8. Particle size distributions, engine pressure ratio 1.3, probe distance 1 m, parameters are fuel sulfur content, and dilution ratio.

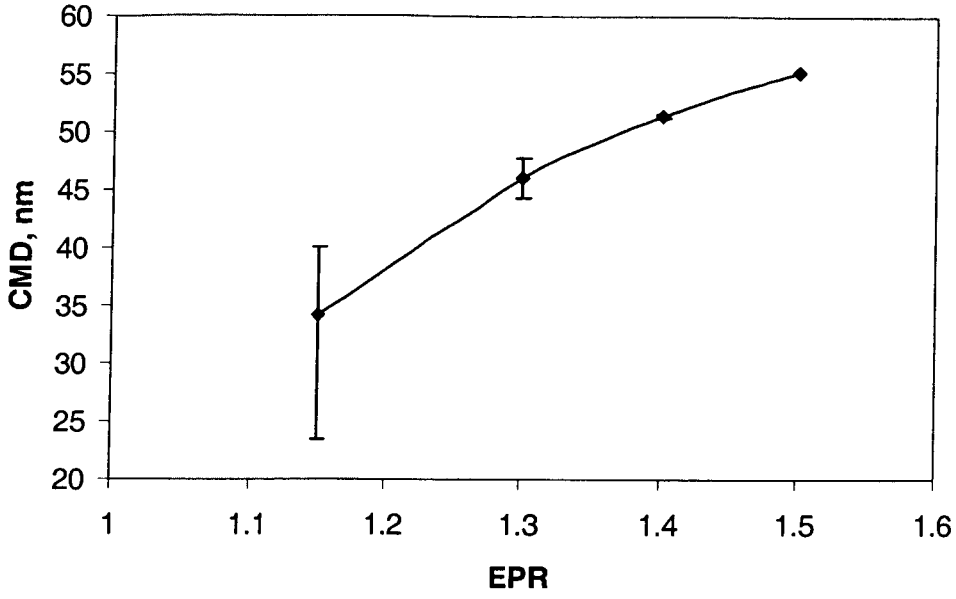

Fig. 9. Change in count mean diameter with engine pressure ratio. Probe distance is 1 m and fuel sulfur content is 1820 ppm. Data are for runs 46, 63, 49, 66,68, 69, and 71.

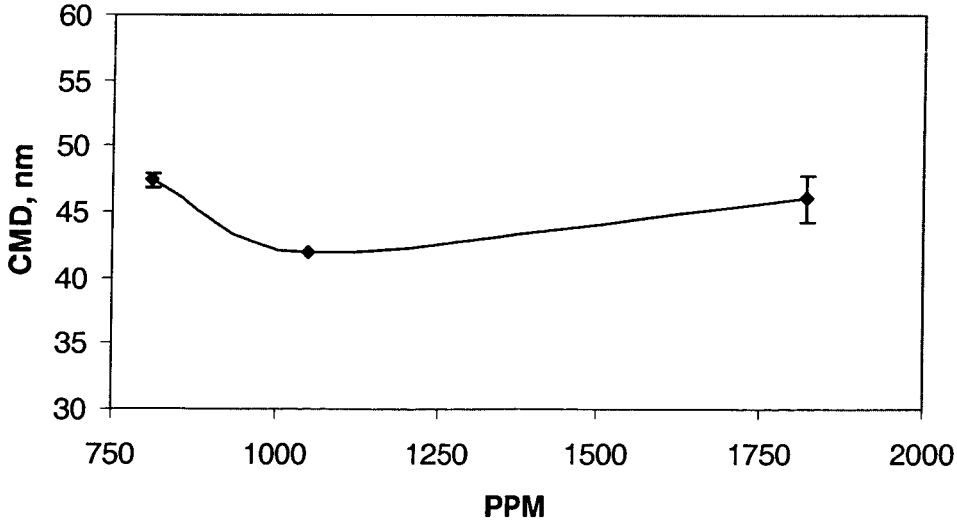

Fig. 10. Change in count mean diameter with fuel sulfur content. Probe distance is 1 m and engine pressure ratio is 1.3. Data are for runs 98, 99, 33, 66, and 49.

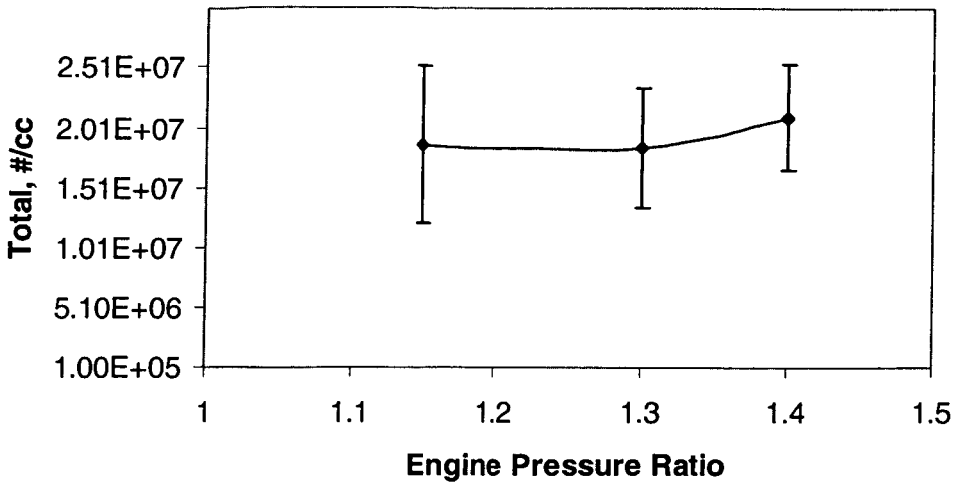

Fig. 11. Change in total particle number density with engine pressure ratio. Total number densities are averages of run 63, 46, 66, 49, 68 and 52.

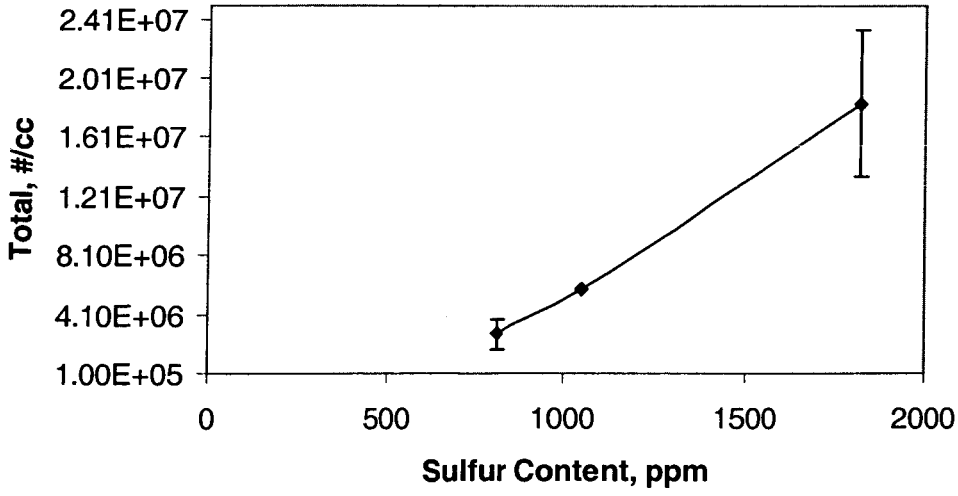

Fig. 12. Change in total particle number density with fuel sulfur content. Total number densities are averages of run 98, 99, 33, 66, and 49.

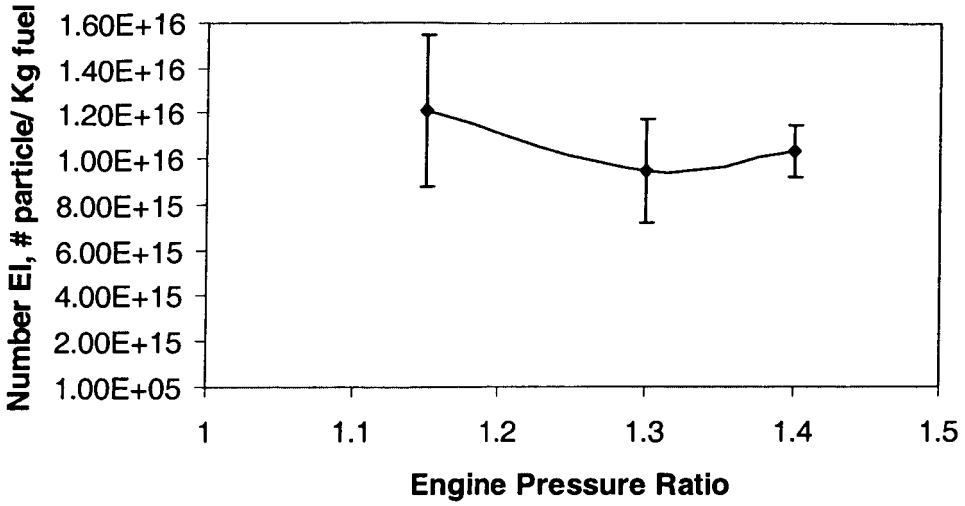

Fig. 13. Change in number based Emissions Index with engine pressure ratio. Probe distance is 1 m and fuel sulfur content is 1820 ppm. Emissions Indices are averages of run 63, 46, 66, 49, 68 and 52.

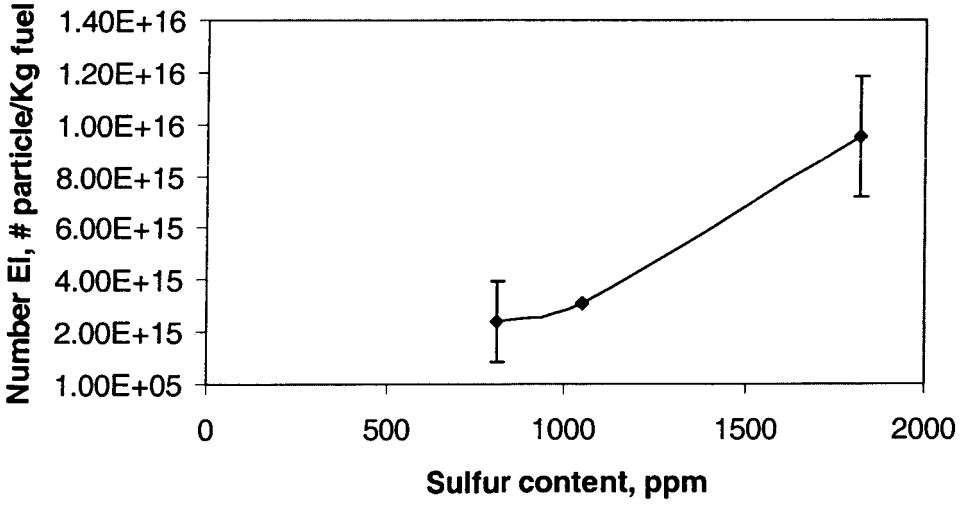

Fig. 14. Change in number based Emissions Index with fuel sulfur content. Probe distance is 1 m and engine pressure ratio is 1.3. Emissions Indices are averages of run 98, 99, 33, 66, and 49.

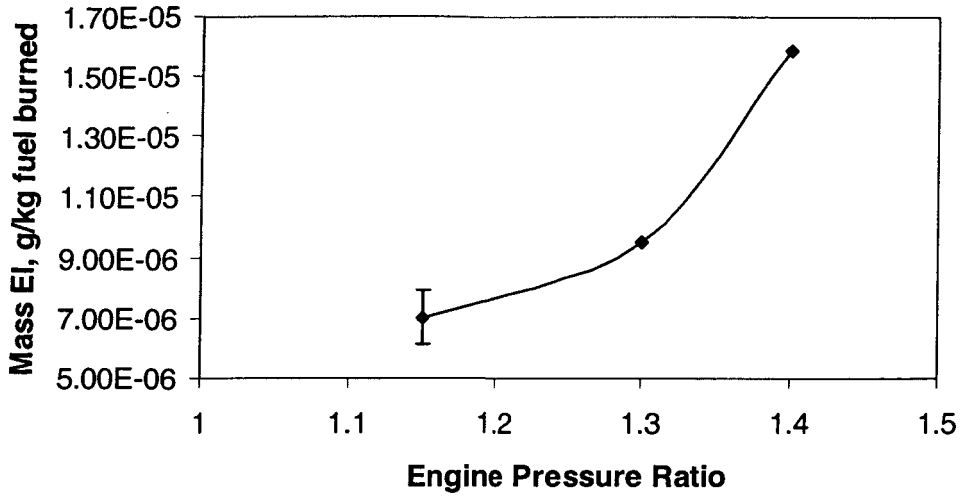

Fig. 15. Change in mass based Emissions Index with engine pressure ratio. Probe distance is 1 m and fuel sulfur content is 1820 ppm. Emissions Indices are averages of run 63, 46, 66, 49, 68 and 52.

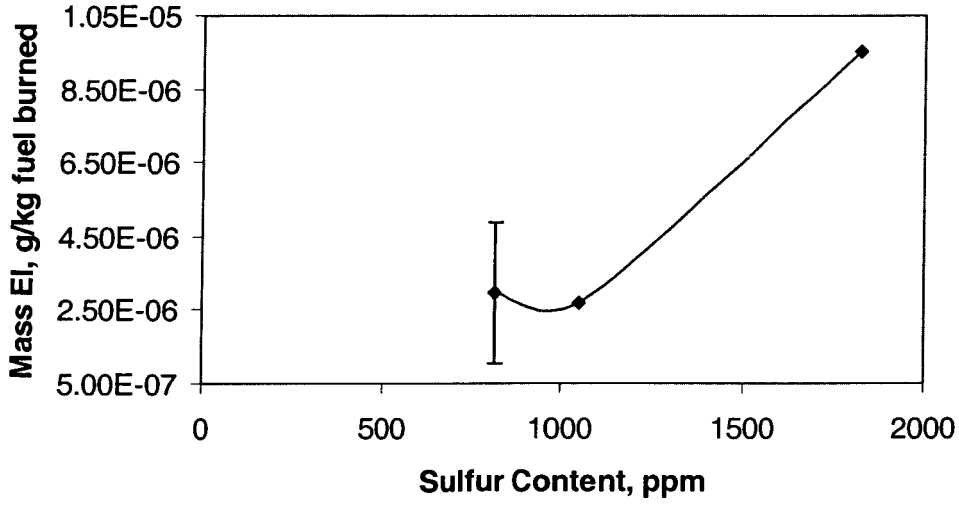

Fig. 16. Change in mass based Emissions Index with fuel sulfur content. Probe distance is 1 m and engine pressure ratio is 1.3. Emissions Indices are averages of run 98, 99, 33, 66, and 49.